PROCEEDINGS, Thirty-Seventh Workshop on Geothermal Reservoir Engineering
Stanford University, Stanford, California, January 30 - February 1, 2012
SGP-TR-194

EXPONENTIAL EULER TIME INTEGRATOR FOR SIMULATION OF GEOTHERMAL PROCESSES IN HETEROGENEOUS POROUS MEDIA

Antoine Tambue[1], Inga Berre[1,2], Jan M. Nordbotten[1,3], Tor Harald Sandve[1]

[1]Dept. of Mathematics, University of Bergen, P.O. Box 7800, N5020 Bergen, Norway
[2]Chrisian Michelsen Research AS, Norway
[3]Dept. of Civil and Environmental Engineering, Princeton University, USA

e-mail: antoine.tambue@math.uib.no

ABSTRACT

Simulation of geothermal systems is challenging due to coupled physical processes in highly heterogeneous media. Combining the exponential Euler time integrator with finite volume (two-point or multi-point flux approximations) space discretizations leads to a robust methodology for simulating geothermal systems. In terms of efficiency and accuracy, the exponential Euler time integrator has advantages over standard time-dicretization schemes, which suffer from time-step restrictions or excessive numerical diffusion when advection processes are dominating. Based on linearization of the equation at each time step, we make use of a matrix exponential function of the Jacobian, which then provides the exact solution in time for the linearized equations. This is at the expense of computing a matrix exponential function of the stiff Jacobian matrix from the space discretization, together with propagating a linearized system. However, using a Krylov subspace technique makes this computation very efficient, and it can also be implemented without explicit computation of the Jacobian. At the same time, the loss of accuracy due to the linearization does not dominate for geothermal processes. The performance of the method compared to standard time-discretization techniques is demonstrated in numerical examples.

1. INTRODUCTION

In the subsurface, geothermal systems for energy production are characterized by coupled hydraulic, thermal, chemical and mechanical processes. To determine the potential of a geothermal site, and decide optimal production strategies, it is important to understand and quantify these processes. Feasible mathematical modeling and numerical simulations can improve the decision making, but multiple interacting processes acting on different scales leads to challenges in solving the coupled system of equations describing the dominant physics.

Standard discretization methods include finite element, finite volume and finite difference methods for the space discretization (see (Císařová, Kopal, Královcová, & Maryška, 2010; Hayba & Ingebritsen, 1994; Ingebritsen, Geiger, Hurwitz, & Driesner, 2010) and references therein), while standard implicit, explicit or implicit-explicit methods are used for the discretization in time. Challenges with the discretization are, amongst others, related to severe time-step restrictions associated with explicit methods and excessive numerical diffusion for implicit methods.

In this paper, we consider a different approach for the temporal discretization based on the Exponential Euler time integrator, which has recently been suggested as an efficient and robust alternative for the temporal discretization for several applications (Tambue, 2010; Tambue, Geiger, & Lord, 2010; Geiger, Lord, & Tambue, 2012; Carr, Moroney, & Turner, 2011).

The mathematical model discussed, consists of a system of partial differential equations that express conservation of mass, momentum, and energy. In addition, the model will entail phenomenological laws describing processes active in the reservoir. Sample laws are Darcy's law for fluid flow with variable density and viscosity, Fourier's law of heat conduction, and those describing the relation between fluid properties (nonlinear fluid expansivity and compressibility) and porosity subject to pressure and temperature variations. The resulting system of equations is highly nonlinear and coupled and requires sophisticated numerical techniques.

Our solution technique is based on a sequential approach, which decouples the mathematical model into two equations. An advantage of this approach is that it allows for specialized solvers for unknowns with different characteristics (Coumou, Driesner, Geiger, Heinrich, & Matthäi, 2006; Geiger, Driesner, Heinrich, & Matthäi, 2006; Geiger, Driesner, Christoph, Heinrich, & Matthäi, 2006) leading to higher efficiency and accuracy compared to solving the system fully coupled. A finite volume method is applied for the space discretization, and the exponential Euler time integrator (EEM) is applied to integrate the systems explicitly in time based on successive linearizations. Our aim is to achieve more efficient solution strategy compared to fully coupled techniques, as the linearized full coupled matrices are often very poorly conditioned such that small time-steps are required (Geiger, Driesner, Heinrich, & Matthäi, 2006)..

EEM is based on linearizing at each time step the stiff ODEs resulting from the space discretization, and then solving the corresponding linear ODEs exactly in time up to the given tolerance in the computation of a matrix exponential function of the Jacobian. As in all exponential integrators schemes, the expense is the computation of a matrix exponential function of stiff matrix from the space discretization (the stiff Jacobian for EEM scheme), which is a notorious problem in numerical analysis; see (Moler & Van Loan, 2003). However, new developments for both Léja points and Krylov subspace techniques have led to efficient methods for computing matrix exponentials; see e.g. (Tambue, 2010; Tambue, Lord, & Geiger, 2010; Carr, Moroney, & Turner, 2011; Hochbruck & Ostermann, 2010) and references therein. The EEM scheme has been applied successively in various applications; e.g., for solving the Richards equation for unsaturated flow (Carr, Moroney, & Turner, 2011).

In this paper, we present the model equations in Section 2, and the finite volume method for spatial discretization in Section 3. The EEM scheme along with its implementation is presented in Section 4. In this section, we also review the standard θ −Euler methods for the temporal discretization, which will be applied for comparison. In Section 5 we present some numerical examples and comparisons to standard approaches, before we draw some conclusions in Section 6.

2. MODEL EQUATIONS

Throughout all this work we assume that the fluid is water in the single-phase regime. This assumption reduces substantially the complexity of the problem, allowing the energy equation to be written in terms of temperature. However, the same approach as we suggest herein can also be applied for models allowing for phase changes. The model equations are given by (see (Nield & Bejan, 2006; Coumou, Driesner, Geiger, Heinrich, & Matthäi, 2006))

$$\begin{aligned}(1-\phi)\rho_s c_{ps}\frac{\partial T_s}{\partial t} &= (1-\phi)\nabla\cdot(\mathbf{k}_s\nabla T_s)\\ &\quad + (1-\phi)q_s + h_e(T_f - T_s),\\ \phi\rho_f c_{pf}\frac{\partial T_f}{\partial t} &= \phi\nabla\cdot(\mathbf{k}_f\nabla T_f) - \nabla\cdot(\rho_f c_p \mathbf{v} T_f)\\ &\quad + \phi q_f + h_e(T_s - T_f),\end{aligned} \tag{1}$$

where ϕ is the porosity, h_e is the heat transfer coefficient, q is the heat production, ρ is the density, c_p stand for heat capacity, T is the temperature, k is the thermal conductivity with the subscripts f and s referring to fluid and rock, and **v** is the Darcy velocity given by

$$\mathbf{v} = -\frac{\mathbf{K}}{\mu}(\nabla p - \rho_f \mathbf{g}), \tag{2}$$

where **K** is the permeability tensor, μ is the viscosity, **g** is the gravitational acceleration and p the pressure. The mass balance equation for a single-phase fluid is given by

$$\frac{\partial \phi\rho_f}{\partial t} = -\nabla\cdot(\mathbf{v}\rho_f) + Q_f, \tag{3}$$

where Q_f[kg/s] is a source or sink term.
Assuming that the compressibility of the rock is orders of magnitude lower than that of the fluid or the time variation of the porosity is low yields, by use of equation (2)

$$\phi\frac{\partial \rho_f}{\partial t} = \nabla\cdot\left(\frac{\rho_f\mathbf{K}}{\mu}(\nabla p - \rho_f\mathbf{g})\right) + Q_f. \tag{4}$$

Notice that

$$\begin{aligned}\frac{\partial \rho_f}{\partial t} &= \frac{\partial \rho_f}{\partial T_f}\frac{\partial T_f}{\partial t} + \frac{\partial \rho_f}{\partial p}\frac{\partial p}{\partial t}\\ &= \rho_f\left(-\alpha_f\frac{\partial T_f}{\partial t} + \beta_f\frac{\partial p}{\partial t}\right).\end{aligned} \tag{5}$$

Where α_f and β_f are, respectively, the thermal fluid expansivity and its compressibility defined by

$$\alpha_f = -\frac{1}{\rho_f}\frac{\partial \rho_f}{\partial T_f}, \quad \beta_f = \frac{1}{\rho_f}\frac{\partial \rho_f}{\partial p}. \tag{6}$$

Inserting equation (6) in equation (4) yields

$$\phi\rho_f\left(-\alpha_f\frac{\partial T_f}{\partial t} + \beta_f\frac{\partial p}{\partial t}\right) = \tag{7}$$

$$\nabla \cdot \left(\frac{\rho_f \mathbf{K}}{\mu} \left(\nabla p - \rho_f \mathbf{g} \right) \right) + Q_f$$

The state functions μ, ρ_f, c_{pf}, α_f and β_f can be found in (Haar, Gallagher, & Kell, 1982; Fine & Millero, 1973).

The model problem is therefore to find the function (T_s, T_f) satisfying the highly nonlinear equations (1) and (7) subject to (3).

Notice that if $h_e \to \infty$, we have the equilibrium state of the heat and therefore $T_s = T_f$.

3. SPATIAL DISCRETIZATION

For discretization in space, we use the finite volume method on a structured mesh $\mathcal{T}$ (Eymard, Gallouet, & Herbin, 2000; Aavatsmark, 2007) with maximum mesh size $h_{\mathcal{T}}$.

We denote by $\{\Omega_i\}$ the family of control volumes forming the mesh $\mathcal{T}$. The finite volume method space discretization consists of the following steps:

1) Integrate each equations of Eq. (1) and Eq. (7) over each control volume Ω_i.
2) Use the divergence theorem to convert the volume integral into the surface integral in all divergence terms,
3) Use two-point or multi-point flux approximations (useful for unstructured mesh and anisotropic media) for diffusion heat and flow fluxes (Eymard, Gallouet, & Herbin, 2000; Aavatsmark, 2007):

$$f_i^1 = \int_{\partial\Omega_i} \mathbf{n}_i \cdot (k_s \nabla T_s) ds,$$

$$f_i^2 = \int_{\partial\Omega_i} \mathbf{n}_i \cdot \left(k_f \nabla T_f \right) ds, \tag{8}$$

$$f_i^3 = \int_{\partial\Omega_i} \mathbf{n}_i \cdot \left(\frac{\rho_f \mathbf{K}}{\mu} \nabla p \right) ds.$$

4) Use the standard upwind weighting (Eymard R. 2000) for the convective (advective) flux

$$f_i^4 = \int_{\partial\Omega_i} \mathbf{n}_i \cdot \left(\rho_f c_{pf} T_f \mathbf{v} \right) ds. \tag{9}$$

Reorganizing these space approximations yield the following system of stiff ODEs:

$$\begin{aligned} \frac{dT_s^h}{dt} &= G_1\left(T_s^h, T_f^h, t\right), \\ \frac{dT_f^h}{dt} &= G_2\left(T_s^h, T_f^h, p_h, t\right), \end{aligned} \tag{10}$$

$$\frac{dp_h}{dt} = G_3\left(p_h, T_f^h, t\right) + \frac{\alpha(T_f^h, p_h)}{\beta(T_f^h, p_h)} \cdot \frac{dT_f^h}{dt}.$$

Here, the discretized dependent variables are denoted with the superscript h. Letting

$$T_h = (T_s^h, T_f^h)^T, \tag{11}$$

this system can be rewritten as

$$\frac{dT_h}{dt} = G(T_h, p_h, t), \tag{12}$$

$$\begin{aligned} \frac{dp_h}{dt} &= G_3\left(p_h, T_f^h, t\right) + \frac{\alpha\left(T_f^h, p_h\right)}{\beta\left(T_f^h, p_h\right)} \\ &\quad \cdot G_2\left(T_s^h, T_f^h, p_h, t\right) \\ &= G_4(T_h, p_h, t), \end{aligned} \tag{13}$$

where

$$\begin{aligned} &G(T_h, p_h, t) = \\ &\left(G_1\left(T_s^h, T_f^h, t\right), G_2\left(T_s^h, T_f^h, p_h, t\right) \right)^T. \end{aligned} \tag{14}$$

For a given initial pressure $p_h(0)$ (giving a corresponding initial velocity $\mathbf{v}_h(0)$) and initial temperature $T_h(0)$ the technique used in this work consists of solving successively the systems (12) and (13), given $p_h(0)$ and $T_h(0)$.

4. TEMPORAL DISCRETIZATIONS

θ-Euler Schemes

In the following, we briefly describe the standard integrators that we will use in this paper for comparison with exponential integrator.

Consider the stiff ODEs Eq. (12) and Eq. (13) within the interval $[0, \tau], \tau > 0$. Given a time-step $\Delta t_n = t^{n+1} - t^n$, applying the θ-Euler scheme with respect to the function T_h in the ODEs (11) yields

$$\begin{aligned} \frac{T_h^{n+1} - T_h^n}{\Delta t_n} &= \theta G(T_h^{n+1}, p_h^n, t^{n+1}) \\ &\quad + (1-\theta) G(T_h^n, p_h^n, t^n). \end{aligned} \tag{15}$$

$T_h(0) = T^0, \quad 0 \le \theta \le 1.$

For $\theta \neq 0$, the scheme is implicit and given the approximation solutions T_h^n and p_h^n at time t^n, the solution T_h^{n+1} at time t^{n+1} is obtained by solving the nonlinear equation

$$\begin{aligned} \mathcal{F}(X) &= X - \theta \Delta t_n G \ \ (T_h^{n+1}, p_h^n, t^{n+1}) \\ &\quad + \Delta t_n (1-\theta) G(T_h^n, p_h^n, t^n) - T_h^n, \\ X &= T_h^{n+1}, \end{aligned} \tag{16}$$

which is solved using the Newton method. For efficiency, all linear systems are solved using the Matlab function bicgstab with ILU(0) preconditioners, which are updated at each time step..

To solve the ODEs (13) we apply again the θ-Euler method, but with respect to p_h, which yields

$$\begin{aligned}\frac{p_h^{n+1}-p_h^n}{\Delta t_n} &= \theta G_4(T_h^n, p_h^{n+1}, t^{n+1}) \\ &+(1-\theta)G_4(T_h^n, p_h^n, t^n), \\ p_h(0) &= p^0, \quad 0 \le \theta \le 1.\end{aligned} \tag{17}$$

For $\theta = 1/2$ the θ-Euler scheme is second order in time and for $\theta \neq 1/2$ the scheme is first order in time. In this paper, the standard sequential approach to solve the ODEs (12)-(13) consists to apply successively the schemes (15) and (17).

Exponential Euler Method

To introduce the Exponential Euler Method let us first consider the following system of stiff ODEs, which commonly follows from space discretization of semilinear parabolic PDEs:

$$\begin{aligned}\frac{d\mathbf{y}}{dt} &= \mathbf{L}\mathbf{y} + \mathbf{g}(\mathbf{y}, t), t \in [0, \tau]. \\ \boldsymbol{y}(0) &= \mathbf{y}^0.\end{aligned} \tag{18}$$

Here **L** is a stiff matrix and **g** a nonlinear function.
This allows us to write the exact solution of (18) as

$$\boldsymbol{y}(t^n) = e^{t^n\mathbf{L}}\mathbf{y}^0 + \int_0^{t^n} e^{(t^n-s)\mathbf{L}}\mathbf{g}(\mathbf{y}(s), s)ds. \tag{19}$$

Given the exact solution at the time t^n we can construct the corresponding solution at t^{n+1}as

$$\begin{aligned}\boldsymbol{y}(t^n) &= e^{\Delta t_n\mathbf{L}}\mathbf{y}(t^n) \\ &+\int_0^{\Delta t_n} e^{(\Delta t_n-s)\mathbf{L}}\mathbf{g}(\mathbf{y}(t^n+s), t^n+s)ds.\end{aligned} \tag{20}$$

Note that the expression in (20) is still an exact solution. The idea behind Exponential Time Differencing (ETD) is to approximate $\mathbf{g}(\mathbf{y}(t^n + s), t^n + s)$ by a suitable polynomial (see (Cox S. M. and Matthews P. C., 2002)), the simplest is given by $\mathbf{g}(\mathbf{y}(t^n + s), t^n + s) \approx \mathbf{g}(\mathbf{y}(t^n), t^n)$ with the corresponding ETD1 scheme given by

$$\begin{aligned}\mathbf{y}^{n+1} &= e^{\Delta t_n\mathbf{L}}\mathbf{y}^n \\ &+\Delta t_n\varphi_1(\Delta t_n\mathbf{L})\big(\mathbf{L}\mathbf{y}^n + \mathbf{g}(\mathbf{y}^n, t^n)\big),\end{aligned} \tag{21}$$

where

$$\varphi_1(A) = \sum_{i=1}^{\infty}\frac{A^{i-1}}{i!} = A^{-1}(e^A - I), \tag{22}$$

and the second equality is used when A is invertible. The ETD1 scheme in Eq. (21) can be rewritten as

$$\begin{aligned}\mathbf{y}^{n+1} &= \mathbf{y}^n \\ &+\Delta t_n\varphi_1(\Delta t_n\mathbf{L})\big(\mathbf{L}\mathbf{y}^n + \mathbf{g}(\mathbf{y}^n, t^n)\big).\end{aligned} \tag{23}$$

This new expression has the advantage that it is computationally more efficient as only one matrix exponential function needs to be evaluated at each step.

Recently, ETD1 scheme was applied to advection-dominated reactive transport in heterogeneous porous media (Tambue, Lord, & Geiger, 2010; Tambue, 2010; Geiger, Lord, & Tambue, 2012). A rigorous convergence proof in the case for a finite volume space discretization is presented in (Tambue, 2010; Tambue, 2011). In these works, it was observed that the exponential methods were generally more accurate and efficient than standard implicit methods.

As our systems (12) and (13) are highly nonlinear, we need to linearize before applying ETD1 scheme.
Consider the system (12) of ODEs. For simplicity we assume that it is autonomous

$$\begin{aligned}\frac{dT_h}{dt} &= G(T_h, p_h), \\ T_h(0) &= T^0.\end{aligned} \tag{24}$$

To obtain the numerical approximation T_h^{n+1} of the exact solution, we linearize $G(T_h, p_h)$ at T_h^n and obtain the following semilinear ODEs:

$$\begin{aligned}\frac{dT_h}{dt} &= \mathbf{J}_n T_h(t) + \mathbf{g}(T_h(t), p_h^n), \\ t^n &\le t \le t^{n+1},\end{aligned} \tag{25}$$

where $\mathbf{J}_n$ denotes the Jacobian of the function G with respect to T_h and **g** the remainder given by

$$\begin{aligned}\mathbf{J}_n &= D_{T_h}G(T_h^n, p_h^n), \\ \mathbf{g}(T_h(t), p_h^n) &= G(T_h(t), p_h^n) - \mathbf{J}_n T_h(t),\end{aligned} \tag{26}$$

Applying the ETD1 scheme to (24) yields

$$T_h^{n+1} = T_h^n + \Delta t_n\varphi_1(\Delta t_n\mathbf{J}_n)\,G(T_h^n, p_h^n) \tag{27}$$

This method is typically denoted the Exponential Euler method (EEM) or exponential Rosenbrock-Euler method (Caliari M. and Ostermann A., 2009), and has been reinvented a number of times in different names (see (Carr, Moroney, & Turner, 2011) for more references).

For simplicity, the EEM scheme (27) is applied for autonomous problems here. The EEM scheme is second order in time (Carr, Moroney, & Turner, 2011; Caliari M. and Ostermann A., 2009). To deal with non-autonomous problems while conserving the second order accuracy of the EEM scheme, one needs to convert to autonomous problems first (see (Caliari M. and Ostermann A., 2009) for more details about such transformations).

To solve the ODEs (13) we again apply the EEM scheme, but with respect to p_h, which yields

$$p_h^{n+1} = p_h^n + \Delta t_n \varphi_1(\Delta t_n \mathcal{J}_n) G_4(T_h^n, p_h^n), \qquad \mathcal{J}_n = D_{p_h} G_4(T_h^n, p_h^n). \tag{28}$$

As with θ-Euler methods, the sequential approach proposed in this paper consists in solving the ODEs (12)-(13) successively, applying the schemes (27) and (28).

Implementation of the EEM Scheme

The key element in the exponential integrators schemes is the computation of the matrix exponential functions, the so-called φ_i-functions. There are many techniques available (Hochbruck & Ostermann, 2010). Some techniques, like standard Padé approximation, compute the whole matrix exponential functions at every time step, and are, therefore, memory and time consuming for large problems. For such problems, the Krylov subspace technique and the real fast Leja points technique have proved to be efficient (Tambue, 2010; Tambue, Geiger, & Lord, 2010; Carr, Moroney, & Turner, 2011). In the current work, we use the Krylov subspace technique.

Krylov subspace technique

For a given Krylov dimension m, the main idea of the Krylov subspace technique is to approximate the action of the exponential matrix function $\varphi_1(\Delta t_n \mathbf{J}_n)$ on a vector $\mathbf{v}$ by projecting it onto a small Krylov subspace $K_m = \text{span}\{\mathbf{v}, \mathbf{J}_n\mathbf{v}, \dots, (\mathbf{J}_n)^{m-1}\mathbf{v}\}$. The approximation is formed using an orthonormal basis $\mathbf{V}_m = [\mathbf{v}_1, \mathbf{v}_2, \dots, \mathbf{v}_m]$ of the Krylov subspace K_m and of its completion $\mathbf{V}_{m+1} = [\mathbf{V}_m, \mathbf{v}_{m+1}]$. The basis is found by Arnoldi iteration, which uses stabilized Gram-Schmidt to produce a sequence of vectors that span the Krylov subspace.

Let $\mathbf{e}_i^j$ be the i th standard basis vector of $\mathbb{R}^j$. We approximate $\varphi_1(\Delta t_n \mathbf{J}_n)\mathbf{v}$ by

$$\varphi_1(\Delta t_n \mathbf{J}_n)\mathbf{v} \approx |\mathbf{v}|_2 \mathbf{V}_{m+1} \varphi_1(\Delta t_n \bar{\mathbf{H}}_{m+1}) \mathbf{e}_1^{m+1} \tag{29}$$

with

$$\bar{\mathbf{H}}_{m+1} = \begin{bmatrix} \mathbf{H}_m & \underline{0} \\ 0, \dots, 0, h_{m+1,m} & 0 \end{bmatrix} \tag{30}$$

Where

$$\mathbf{H}_m = \mathbf{V}_m^T \mathbf{J}_n \mathbf{V}_m = [h_{i,j}]. \tag{31}$$

The coefficient $h_{m+1,m}$ is recovered in the last iteration of Arnoldi's iteration; see (Tambue, Lord, & Geiger, 2010; Tambue, 2010). For a small Krylov subspace (i.e, m is small) a standard Padé approximation can be used to compute $\varphi_1(\Delta t_n \bar{\mathbf{H}}_{m+1})$, but efficiency is gained by recovering $\varphi_1(\Delta t_n \bar{\mathbf{H}}_{m+1})\mathbf{e}_1^{m+1}$ directly from the Padé approximation of the exponential of a matrix related to $\mathbf{H}_m$ (Sidje R. B. 1998).

Notice that this implementation can be done without explicit computation of the Jacobian matrix $\mathbf{J}_n$ as the Krylov subspace K_m can be formed by using the following approximations:

$$\mathbf{J}_n\mathbf{v} \approx \frac{G(T_h^n + \epsilon\mathbf{v}, p_h^n) - G(T_h^n, p_h^n)}{\epsilon} \tag{32}$$

or

$$\mathbf{J}_n\mathbf{v} \approx \frac{G(T_h^n + \epsilon\mathbf{v}, p_h^n) - G(T_h^n - \epsilon\mathbf{v}, p_h^n)}{2\epsilon}, \tag{33}$$

for a suitably chosen perturbation ϵ as in (Carr, Moroney & Turner 2011). These approximations prove that EEM scheme with the Krylov subspace technique can be implemented using the Jacobian-free technique. The implementation can be done using standard local time errors control and time step subdivision as in many ODEs software. This is, for example, implemented in the function ''phiv'' of the package Expokit (Sidje R. B. 1998) which appears to be the most used package for φ_1-computation applying the Krylov subspace technique. It is available in MATLAB and FORTRAN.

5. NUMERICAL EXAMPLES

We consider a heterogeneous reservoir described by the domain $\Omega = [0,10] \times [0,10] \times [0,1]$, where all distances are in km. The half upper part of the reservoir is less permeable than the lower part. An injection point is located at the position $(10,10,z), z \in [0,1]$, injecting with a rate $q_e = 0.57\, m^3/s$, and the production is at $(0,0,z), z \in [0,1]$ with rate $q_p = 0.001\, m^3/s$. At the injection point we take $\mathrm{q_f} = 10^{-4}\ \mathrm{W/(m^3)}$.

Homogeneous Neumann boundary conditions are applied for both the pressure equation given by the mass conservation law and the energy equation. The half upper part of the reservoir has rock properties:

permeability $K = 10^{-2}\, Darcy$, porosity $\phi = 20\%$, $\rho_s = 2800\, kg/m^3, c_{ps} = 850\, J/(kg.K)$, k_s= 2W/(m.K) while rock proprieties of the half lower part are : $K = 10^{-1}\, Darcy$, $\phi = 40\%$, $\rho_s = 3000\, Kg/m^3, c_{ps} = 1000\, J/(kg.K)$, k_s= 3W/(m.K). Here we deal with temperature between 0 and 100℃ and pressure less than $100MPa$. The water thermal expansivity α_f and its compressibility β_f used can found in (Fine & Millero, 1973). For simplicity, we assume that ρ_f, μ are only function of temperature as in (Graf, 2009) and, further, that $c_{pf} = 4200 J/(kg.K)$, $k_f = 0.6\, W/(m.K)$.

All our tests were performed on a workstation with a 3 GHz Intel processor and 8 GB RAM. Our code was implemented in Matlab 7.11. We also used part of the codes in (Lie, Krogstad, Ligaarden, Natvig, Nilsen, & Skaflestad, 2011) for space discretization.

The initial temperature at $z = 0$ is set to 50℃ and the temperature increases 3℃ every 100 m. The initial pressure can be the steady state pressure with water proprieties at the initial temperature or the hydrostatic pressure. We take the heat transfer coefficient h_e sufficiently large to reach to local equilibrium.

In our simulations, we used $0.4 \times 0.4 \times 0.05$ uniform grid. The Krylov dimension used in EEM scheme is $m = 10$. The absolute tolerance in both Krylov subspace technique and Newton iterations is $tol = 10^{-6}$.

Figure 1 shows the temperature field at time $\tau = 4$ days, while Figure 2 shows the temperature field at $\tau = 20$ days. In Figure 3 we plot the L^2 norm of the relative errors of temperature versus time step size at the final time $\tau = 4\, days$. This figure shows the convergence for both the standard scheme denoted by 'Implicit' and the EEM scheme denoted by 'EEM'. Here we use $\theta = 1/2$ in the standard θ-Euler schemes. The reference solution used in the errors calculations is the numerical solution with smaller time step size.

Figure 3 shows also that the EEM scheme is more accurate than the standard θ-Euler scheme in this example. We observe the order reduction in both schemes due to splitting. The order of convergence for EEM scheme is order 1.15 in time while the order for the θ-Euler method is 1.05.

Figure 4 shows the CPU time versus the L^2 norm of the relative errors. We can observe the high efficiency of the EEM scheme over the standard θ-Euler scheme.

Figure 5 shows the time step size versus the CPU time. We can observe that the EEM scheme is three times as efficient as the standard theta Euler scheme. This is perhaps surprising and certainly encouraging. Similar performance have been reached in (Carr, Moroney, & Turner, 2011) by solving the Richards equation for unsaturated flow and overcame in (Caliari, Vianello, & Bergamaschi, 2007), where a similar scheme have been shown to be up to five time faster than a classical second-order implicit solver with ILU(0) precondictioners for advection-diffusion-reaction equation with the real fast Leja points technique in exponential matrix computation.

6. CONCLUSION

We have proposed a novel approach for simulation of geothermal processes in heterogeneous porous media. This approach uses the exponential integrator scheme EEM, decouples the mass conservation equation from the energy equation and solves each stiff ODEs from space discretization sequentially.

Numerical simulation shows that using the Krylov subspace technique in the computation of the exponential function φ_1 in EEM scheme makes our approach more efficiency and accurate compared to the second order Crank–Nicolson method (1/2 - Euler method).

ACKNOWLEDGEMENTS

This work was funded by the Research Council of Norway (grant number 190761/S60).

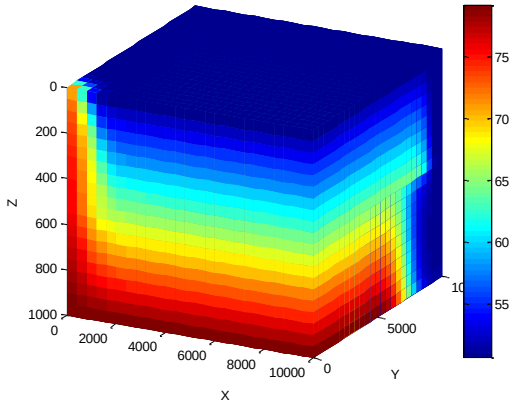

Figure 1: Temperature field at the final time $\tau =$ 4 *days.*

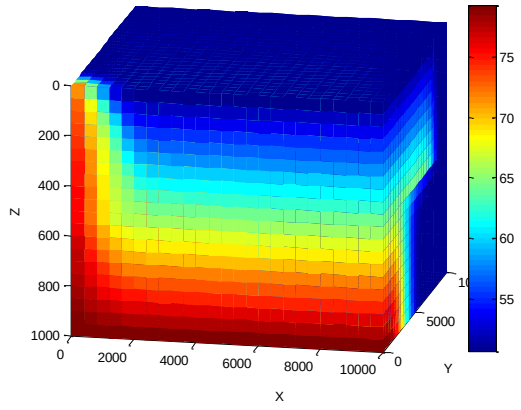

Figure 2: Temperature field at the final time $\boldsymbol{\tau} =$ 20 *days.*

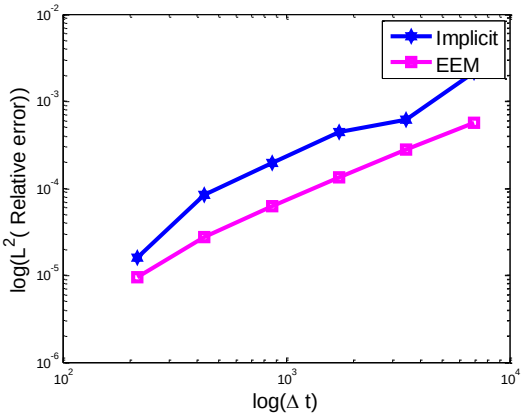

Figure 3: The L^2 *norm of the relative errors of the temperature T versus time step size at the final time* $\tau = 4$ *days.*

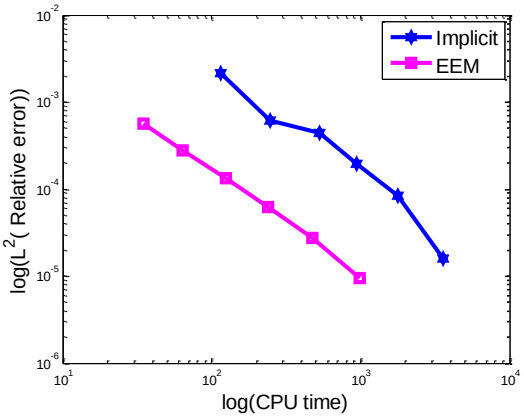

Figure 4: The CPU time versus the L^2 *norm of the relative errors corresponding to Figure 3.*

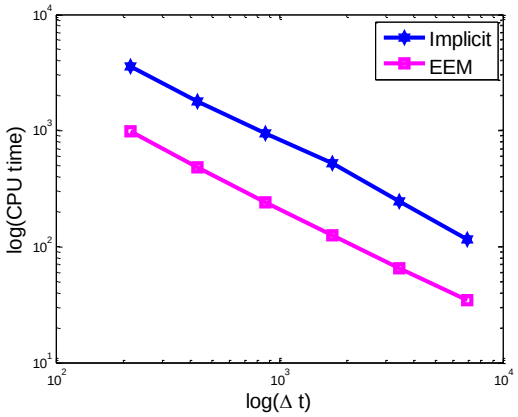

Figure 5: The time step size versus the CPU time corresponding to Figure 3.

REFERENCES

Aavatsmark, I. (2007). Multipoint flux approximation methods for quadrilateral grids. *9th International Forum on Reservoir Simulation.* Abu Dhabi.

Caliari M. and Ostermann A. (2009). Implementation of exponential Rosenbrock-type integrators. *Applied Numerical Mathematics*, 568-581 (59).

Caliari, M., Vianello, M., & Bergamaschi, L. (2007). The LEM exponential integrator for advection-diffusion-reaction equations. *Journal of Computational and Applied Mathematics*, 210 (1-2)56-63.

Carr, E. J., Moroney, T. J., & Turner, I. W. (2011). Efficient simulation of unsaturated flow using exponential time integration. *Applied Mathematics and Computation*, 217(14) , p. 6587.

Císařová, K., Kopal, J., Královcová, J., & Maryška, J. (2010). Simulation of geothermal processes. *Proceedings World Geothermal Congress.* Bali, Indonesia.

Coumou, D., Driesner, T., Geiger, S., Heinrich, C. A., & Matthäi, S. (2006). The dynamics of mid-ocean ridge hydrothermal systems: Splitting plumes and fluctuating vent temperatures. *Earth and Planetary Science Letters*, 245, p 218–231.

Cox S. M. and Matthews P. C. (2002). Exponential time differencing for stiff systems. *J. Comput. Phys. 176(2)*, 430-455.

Eymard, R., Gallouet, T., & Herbin, R. (2000). Finite volume methods. In a. L. P. G. Ciarlet P. G., *Handbook of Numerical Analysis* (pp. pp. 713–1020). North-Holland, Amsterdam.

Fine, R. A., & Millero, F. J. (1973). Compressibility of water as a function of temperature and pressure. *J. Chem. Phys. 59, 5529*.

Geiger, S., Driesner, T., Christoph, A., Heinrich, C. A., & Matthäi, S. S. (2006). Multiphase Thermohaline Convection in the Earth's Crust: II. Benchmarking and Applicationof a Finite Element -- Finite Volume Solution Technique with a NaCl–H2O Equation of State. *Transport in Porous Media*, 63:435--461.

Geiger, S., Driesner, T., Heinrich, C. A., & Matthäi, S. K. (2006). Multiphase Thermohaline Convection in the Earth's Crust: I. A New Finite Element -- Finite Volume Solution Technique Combined With a New Equation of State for NaCl–H2O. *Transport in Porous Media*, 63: p. 399--434.

Geiger, S., Lord, G., & Tambue, A. (2012). Exponential time integrators for stochastic partial differential equations in 3D reservoir. *Computational Geosciences*, DOI: 10.1007/s10596-011-9273-z.

Graf, T. (2009). *Simulation of Geothermal Flow in Deep Sedimentary Basins in Alberta.* Alberta Geological Survey.

Haar, L., Gallagher, J., & Kell, G. (1982). *NBS/NRC Steam Tables.* Academic Press.

Hayba, D. O., & Ingebritsen, S. (1994). The computer model HYDROTHERM, a three-dimensional finite--difference model to simulate ground--water flow and heat transport in the temperature range of 0 to 1200 oC. *U.S. Geol. Surv. Water Res. Invest. Report*, 94--12252.

Hochbruck, M., & Ostermann, A. (2010). Exponential integrators. *Acta Numerica*, pp. 209--286.

Ingebritsen, S. E., Geiger, S., Hurwitz, S., & Driesner, T. (2010). Numerical simulation of magmatic hydrothermal. *Rev. Geophys.*,, 48, RG1002, doi:10.1029/2009RG000287.

Lie, A. K., Krogstad, S., Ligaarden, I. S., Natvig, J. R., Nilsen, H. M., & Skaflestad, B. (2011). Open Source MATLAB Implementation of Consistent Discretisations on Complex Grids. *Comput. Geosci.*, DOI: 10.1007/s10596-011-9244-4.

Moler, C., & Van Loan, C. F. (2003). Ninteen dubious ways to compute the exponential of a matrix, twenty-five. *SIAM Review*, 45(1), 3--49.

Nield, D. A., & Bejan, A. (2006). *Convection in Porous Media, Third Edition.* New York: Springer Science+Business Media, Inc.

Sidje R. B. (1998). Expokit: A software package for computing matrix exponentials. *ACM Trans. Math. Softw.*, 24(1), 130–156.

Tambue, A. (2010). *Efficient Numerical Schemes for Porous Media flow.* Ph D Thesis, Heriot-Watt University.

Tambue, A. (2011). Space & time errors estimates for the combined FiniteVolume- Exponential integrator for nonlinear reactive flow. Submitted manuscript.

Tambue, A., Geiger, S., & Lord, G. (2010). Exponential Time Integrators for 3D Reservoir. *ECMOR XII – 12 th European Conference on the Mathematics of Oil Recovery.* Oxford, UK.

Tambue, A., Lord, G., & Geiger, S. (2010). An exponential integrator for advection-dominated reactive transport in heterogeneous porous media. *Journal of Computational Physics*, 229(10),3957--3969.